

Melt-Rheological Properties of PP/EVA Blend

A. K. GUPTA,* B. K. RATNAM, and K. R. SRINIVASAN

Centre for Materials Science and Technology, Indian Institute of Technology, New Delhi-110 016, India

SYNOPSIS

This paper describes a study of melt-rheological properties of the binary blend of isotactic polypropylene (PP) and ethylene-vinyl acetate copolymer (EVA) at varying blending ratios (from 0 to 40 wt % EVA content) and using three samples of EVA containing different vinyl acetate contents (VA %), viz. 9, 12, and 19%. Measurements made on a capillary rheometer at three different temperatures (210, 220, and 230°C) in a shear stress range of 10^4 – 10^6 Pa (shear rate 10^1 – 10^4 s⁻¹) are presented and discussed for the effects of blend composition and shear stress on the flow curves, melt viscosity and melt elasticity. Morphology of the blend studied through scanning electron microscopy revealed distinct differences in size and number density of dispersed EVA droplets, which are discussed in terms of the variation of average size and number density of the dispersed EVA droplets as a function of blend composition and shear stress. Melt-rheological properties and morphology of dispersion are correlated and found quite consistent.

INTRODUCTION

Blending of incompatible polymers for achieving properties suited to particular applications is gaining importance. Performance of such two-phase polymer blends depends mainly upon their morphology that develops during the processing, depending on the melt-rheological properties of the components of the blend.¹⁻⁷ A knowledge of the rheological properties of the melt, as well as the blend morphology, is important for the control of the processing parameters for such multiphase blends and, thus, for making suitable polymer blends for desired end-use applications.

Melt-rheological properties (melt viscosity and melt elasticity) of binary blends of polymers often show nonlinear variations with the blending ratio and show well-defined maxima and/or minima at certain composition ranges.¹⁰⁻¹¹ These maxima and minima have been theoretically interpreted by some authors in terms of the effect of the various parameters, viz. shear stress, ratio of melt viscosities, and ratio of melt elasticities of the individual components, so as to predict the morphology of the dispersed phase at any composition of the blend.¹²⁻¹⁵

The binary blend of isotactic polypropylene (PP) and ethylene-vinyl acetate copolymer (EVA) seems suitable for various applications owing to the modification of properties of PP by incorporation of EVA. Our previous paper¹⁶ reported the role of EVA in the impact modification of PP. This paper presents a study of the melt-rheological properties of the PP/EVA blend in a wide range of blend compositions and using various grades of EVA with the VA content varying from 9 to 19%. Melt-flow data recorded on a capillary rheometer at three different temperatures have been presented as conventional flow curves and their differences with blend composition and temperature are discussed. Variations of melt viscosity and melt elasticity with shear stress and blend composition are presented and the features observed in these variations are interpreted in terms of the morphology of the dispersed phase. Scanning electron microscopic study of the morphology of dispersion is carried out at various blend compositions and at varying shear stress for any particular composition.

EXPERIMENTAL

Materials

The isotactic PP used was Koylene M-0030 (MFI = 10), a product of Indian Petrochemicals Corpo-

* To whom correspondence should be addressed.

ration Ltd. The EVA containing 12 wt % vinyl acetate (VA) was ELVAX 3134 (MFI = 8), a product of DuPont. The other two EVA samples containing 9 and 19% VA were the products of U.S.I. Chemical Co. The three samples are abbreviated as EVA-9, EVA-12, and EVA-19, where the number indicates the VA content in wt %.

Preparation of Blends

PP/EVA blends were prepared by melt-mixing the component polymers, in the requisite ratios, in a single-screw extruder (Betol BM-1820) at a screw speed of 30 rpm and temperature range of 200–215°C from the first zone to the die. The strands obtained from the extruder were cut into small granules in a granulator and used for rheological measurements. The blend composition range studied was 0–40 % EVA content. Since this type of blend is generally used for impact toughening of PP, higher EVA contents were not studied.

Measurements

Melt-rheological measurements were carried out on a piston-type capillary rheometer (Goettfert Werkstoff Pruefmaschinen-Rheograph 2001, Version

9.6). The capillary was of a circular cross section (diameter 1 mm) and length/diameter ratio was 30. The apparent shear stress and shear rate obtained from the rheometer using the conventional expressions were corrected by using Bagley and Rabinowitsch corrections as per the procedures described elsewhere.^{2,10}

Morphology of the freeze-fractured extrudate cross sections were studied using a scanning electron microscope (Stereoscan S360) of Cambridge Instruments Ltd.

RESULTS AND DISCUSSION

Flow Curves

The flow curves, shear stress vs. shear rate plots, of the PP/EVA-12 blend at various compositions and its individual components, PP and EVA-12, at 210°C are shown in Figure 1. The effect of VA % of the EVA at a constant blending ratio and temperature on the flow curve is illustrated as set A in Figure 2, while the effect of temperature on the flow curve at a constant blending ratio and constant VA % of the EVA is shown as set B in Figure 2. All the flow

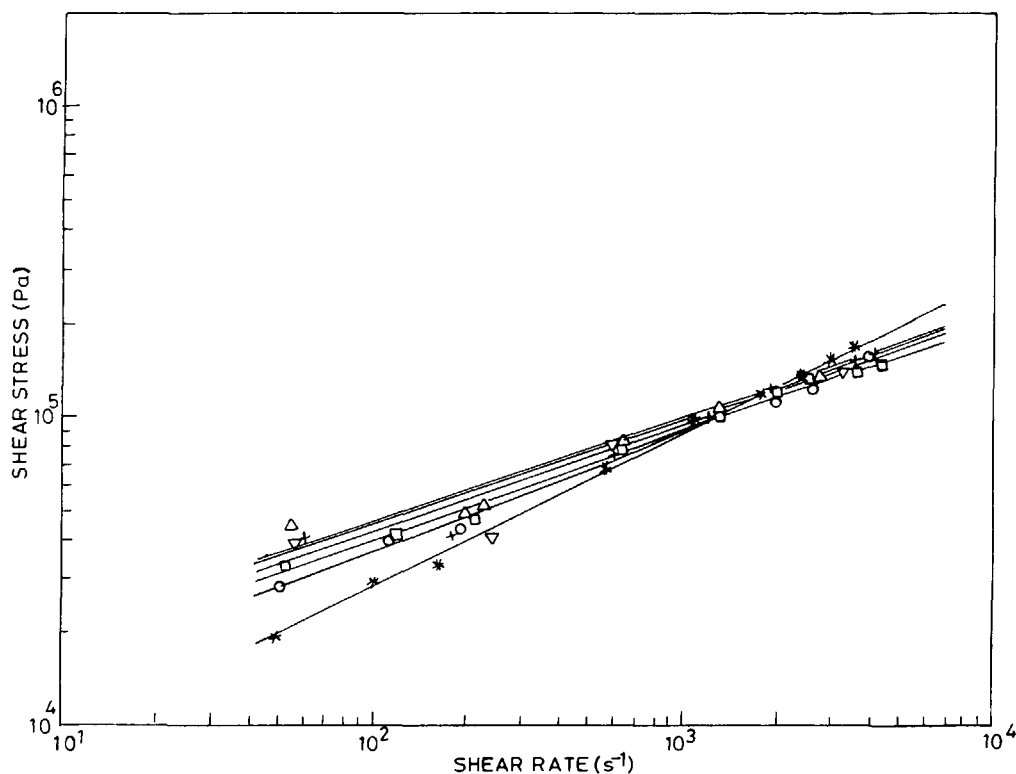


Figure 1 Variation of shear stress with shear rate of (○) PP, (*) EVA, and PP/EVA-12 blend at varying EVA content (wt %): (Δ) 10; (□) 20; (▽) 30; (+) 40.

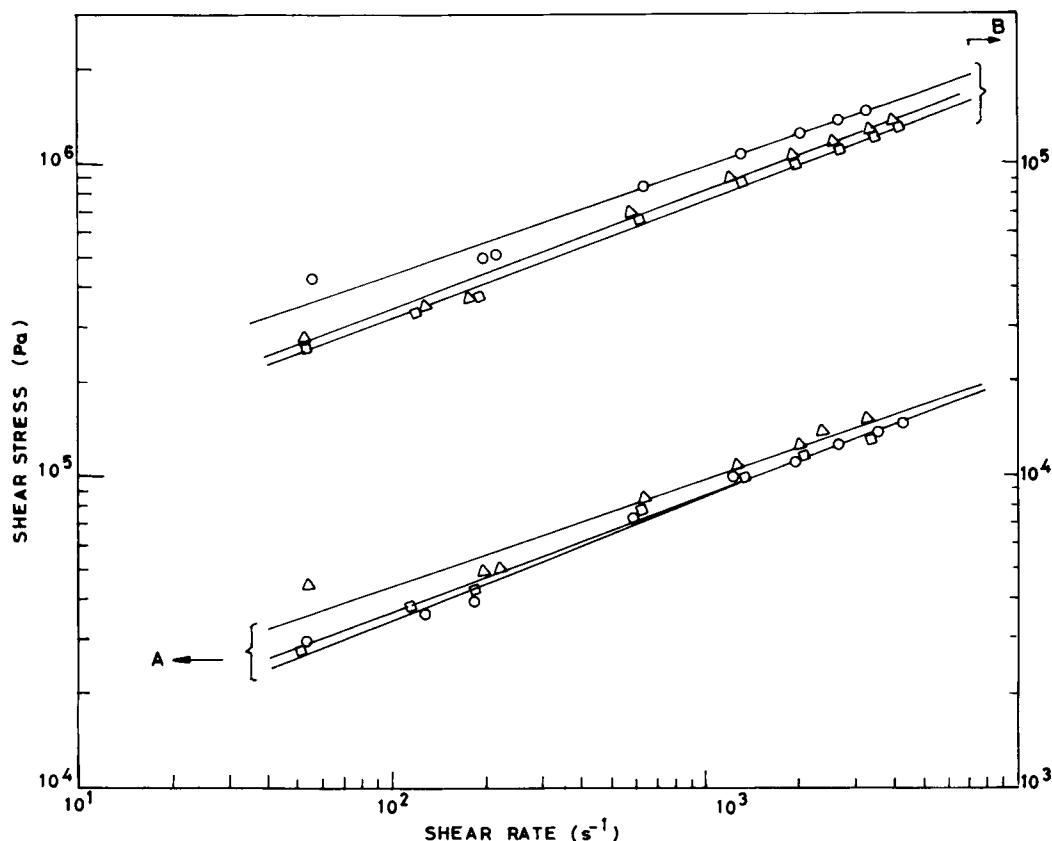


Figure 2 Variation of shear stress with shear rate for (A) PP/EVA at a constant blending ratio (PP/EVA 90/10) of the matrix and varying VA content (wt %) of the EVA used: (○) 9; (△) 12; and (□) 19. (B) PP/EVA-12 (90/10) blend at varying temperature of processing (°C): (○) 210; (△) 220; (□) 230.

curves are quite linear in the studied range of the shear rate, obeying the Ostwald de Waele power law,² $\tau = K\dot{\gamma}^n$, where τ is shear stress; $\dot{\gamma}$, the shear rate; K , the proportionality constant; and n , the power law exponent.

The flow curve of EVA falls distinctly away from those of PP and the blend, both in low- and high-shear rate regions. At low-shear rates (less than $1 \times 10^3 \text{ s}^{-1}$), the flow curve of EVA falls well below that of PP and the blend, while at shear rates greater than $1 \times 10^3 \text{ s}^{-1}$, it lies above them.

Values of the power law exponent " n " evaluated by regression analysis of the data are shown in Table I. The pure components PP and EVA differ quite significantly in their values of n , which is 0.50 for EVA-12 and 0.39 for PP at 210°C. The value of n for the blend is much lower than for both the individual components. Thus, the presence of the dispersed EVA domains seems to increase the pseudoplasticity of the melt. The value of n for the blend samples at 210°C lies in a range 0.30–0.38 without any regular variation with the blending ratio; the value in the middle of the range is somewhat higher.

In the case of pure EVA, variation of n as a function of VA % is nonlinear. n is between 0.50 and 0.58 at 210°C for all the three samples of EVA, indicating their lower pseudoplasticity than that of PP.

With an increase in temperature, the value of n

Table I Values of Power Law Index n

Sample	n		
	210°C	220°C	230°C
PP/EVA-12			
100/0	0.39	0.38	0.41
95/5	0.33	0.38	0.40
90/10	0.32	0.39	0.39
85/15	0.38	0.40	0.39
80/20	0.36	0.41	0.41
70/30	0.38	—	0.43
60/40	0.30	—	0.47
EVA-9	0.53	—	—
EVA-12	0.50	0.52	0.58
EVA-19	0.58	—	—

increases more rapidly for EVA than for PP (seen in Table I). The value of n for the blend, which shows an irregular trend with composition variation at 210°C, in general, increases with increasing EVA content at higher processing temperatures. Thus, the trend of variation becomes more distinctly visible when the disperse phase has a much high value of n than does the matrix.

Melt Viscosity

(a) As a Function of Blend Composition

For the case of a constant VA % (i.e., EVA-12) at a constant temperature (i.e., 210°C), the melt viscosity, η , varies as a function of shear stress and EVA content of the blend, as shown in Figures 3 and 4, respectively. The general trend of decrease of viscosity with increasing shear stress is obeyed by this blend at all the blending ratios, as well as by the two individual components. The slopes, however, differ; the blend and PP show a more rapid decrease of viscosity as a function of shear stress than does EVA. The melt viscosity of the blend at various EVA

contents tends to converge with that of PP at high shear stress. This is apparently the effect of shear forces on the dispersed-phase droplets. As shown in a following section, the droplets are spherical at low shear stress, and as shear stress increases, they tend to deform and orient along the direction of shear. At still higher shear stresses, the elongated droplets tend to break and form small, more or less spherical droplets. Thus, in the high-shear-stress region, owing to the very small size of droplets, which do not modify greatly the melt viscosity, all the blending ratios may have almost the same melt viscosity.

Variation of melt viscosity as a function of the blending ratio is shown in Figure 4 with shear stress as a parameter. The general trend of variation, which is more distinct at low shear stress, is that, initially, the melt viscosity increases with an increase in EVA content of the blend up to 10 wt % and then decreases up to 20 wt % EVA content. Further addition of EVA content shows a gradual increase of melt viscosity. With increasing shear stress, these features gradually disappear and the curve becomes flat, which is consistent with the above-stated decrease in the role of dispersed-phase droplets at high shear.

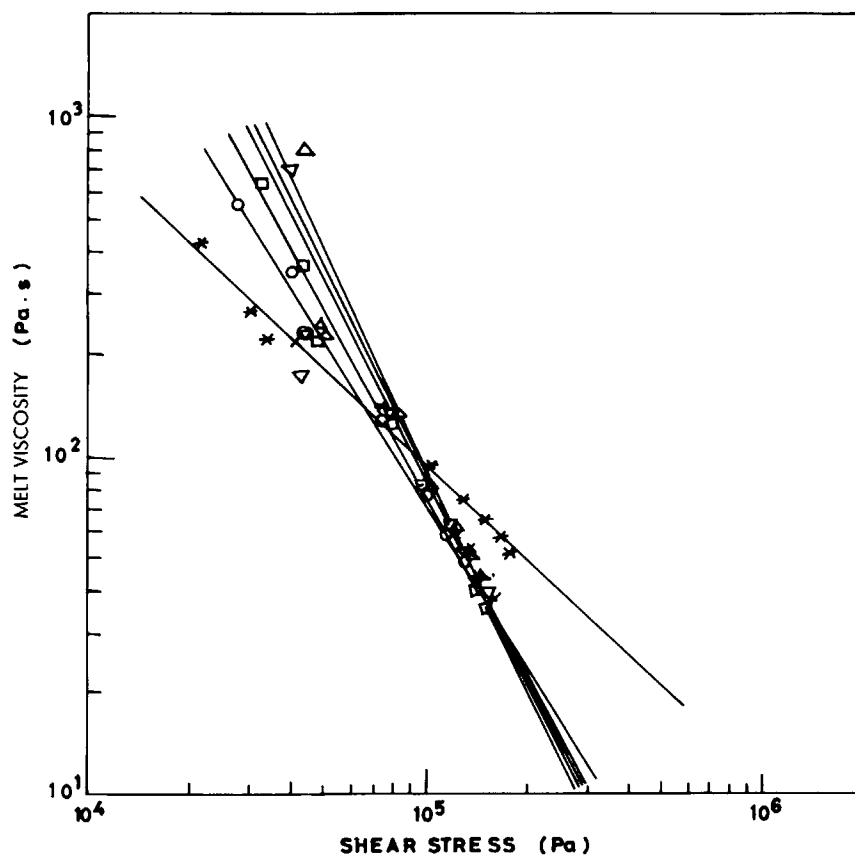


Figure 3 Melt viscosity as a function of shear stress for (○) PP, (*) EVA, and PP/EVA-12 blend at varying EVA content (wt %): (△) 10; (□) 20; (▽) 30; (x) 40.

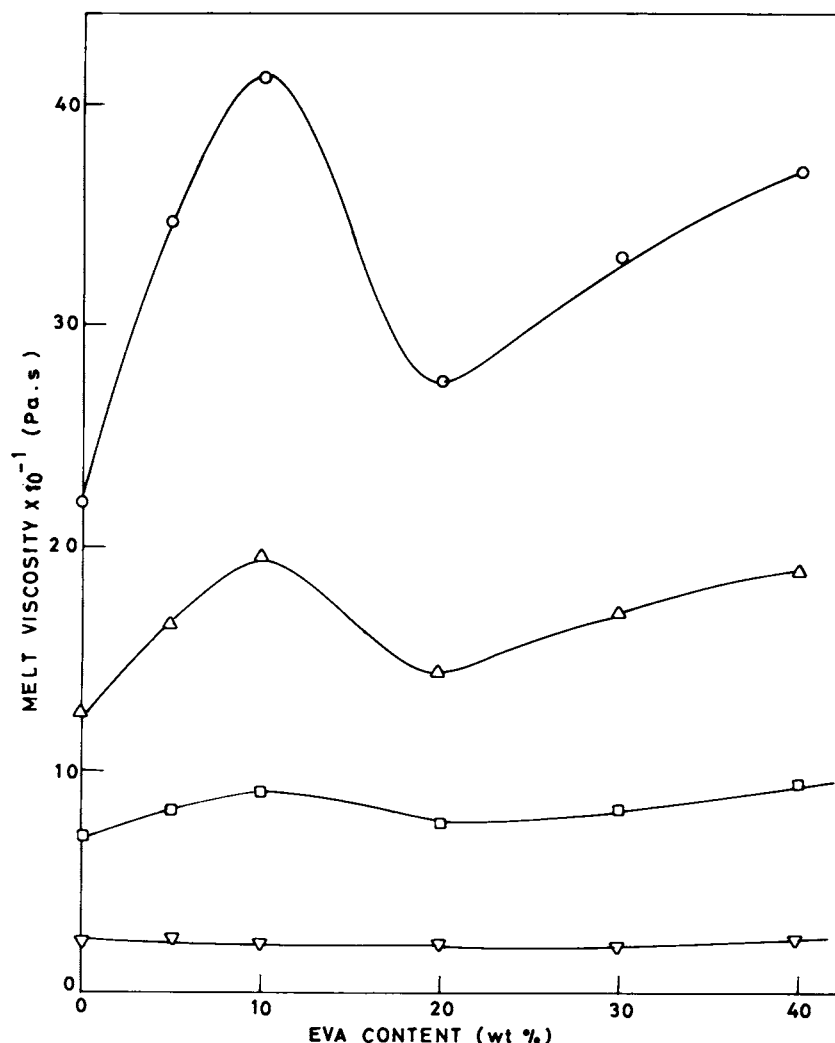


Figure 4 Melt viscosity of PP/EVA-12 blend as a function of EVA content (wt %) with shear stress (Pa) as the variable: (○) 5×10^4 ; (△) 7×10^4 ; (□) 1×10^5 ; (▽) 2×10^5 .

This variation of melt viscosity can be explained on the basis of the variation of the number density and size of the droplets present at the respective compositions of the blend. As will be shown, the morphology of this blend is such that initially up to 10 wt % EVA content the number density of the droplets increases while the variation in diameter is very small, leading to an increase in the value of melt viscosity η . In the region of 10–20 wt % EVA content, the droplet size is higher, and, hence, these droplets can deform more easily since the viscosity of EVA is lower than that of PP, and, consequently, the melt viscosity of the blend in this region decreases. Between the region of 20–30 wt % EVA, the droplet size again decreases with an increasing number density of the droplets and, thus, with a consequent increase of melt viscosity, which increases further in the region 30–40 wt % EVA content.¹ The blend

with 40 wt % EVA content shows rodlike structures of the dispersed-phase domains. The increase of melt viscosity at this composition is attributed to this sudden change in morphology, which might be due to the coalescence of EVA droplets during the processing.

(b) As a Function of Shear Stress

Melt viscosity as a function of shear stress for the case of the blend at 10 wt % EVA-12 content at varying temperatures is shown in Figure 5. The curves are, in general, linear in the shear-stress range studied and the viscosity of the blend decreases with an increase of temperature.

The activation energy for flow calculated from these data using the Arrhenius equation¹⁷ is shown in Table II for PP, EVA, and their binary blend at

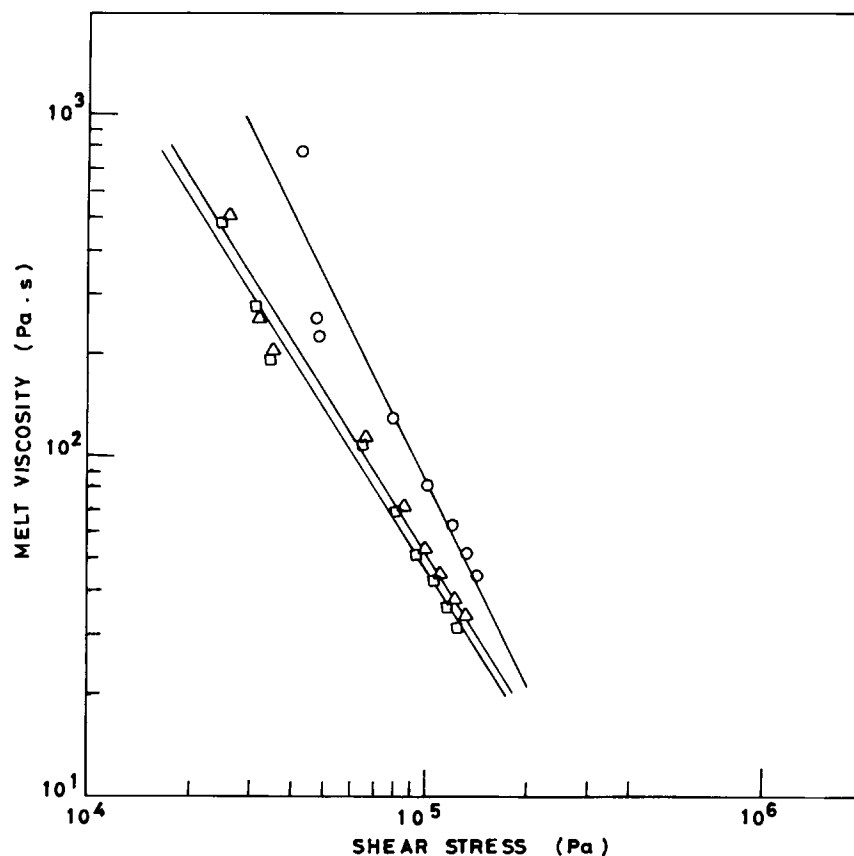


Figure 5 Variation of melt viscosity with shear stress for PP/EVA-12 blend of blending ratio 90/10 at varying temperature of processing ($^{\circ}\text{C}$): (O) 210; (Δ) 220; (\square) 230.

varying compositions. Activation energy increases with increase in EVA content of the blend up to 10 wt %. The activation energy drops with increasing EVA content from about 36 kJ/mol (for 10 wt % EVA content) to 32 kJ/mol (for 20 wt % EVA content). This ease of flow at 20% EVA content seems attributable to easy deformability of the EVA droplets, as this is, incidentally, the composition showing considerably large EVA droplets with respect to those at 10% EVA content. Further increase of EVA content of the blend, beyond 20 wt %, increases the activation energy up to about 52 kJ/mol at 40 wt % EVA content. This variation of activation energy with blending ratio is consistent with the variation of melt viscosity of this system over the entire range studied.

(c) Effect of VA %

The variation of melt viscosity as a function of shear stress at constant EVA content (i.e., 10 wt %) and at constant temperature (i.e., 210 $^{\circ}\text{C}$) with varying

VA % of EVA is shown in Figure 6. The blend with EVA-12 shows higher melt-viscosity than do EVA-9 and EVA-19 at all the shear stresses studied. EVA-9 and EVA-19, on the other hand, show an inappreciable difference in melt viscosity in this range of shear stress. Thus, it seems that VA % of the EVA copolymer has no significant effect on melt viscosity. This observed difference of melt viscosity may be due to the different origin or different molecular

Table II Values of Activation Energy

Blend Composition PP/EVA-12	Activation Energy (kJ/mol)
100/0	28.51
95/5	29.47
90/10	36.87
80/20	32.41
70/38	40.41
60/40	52.76

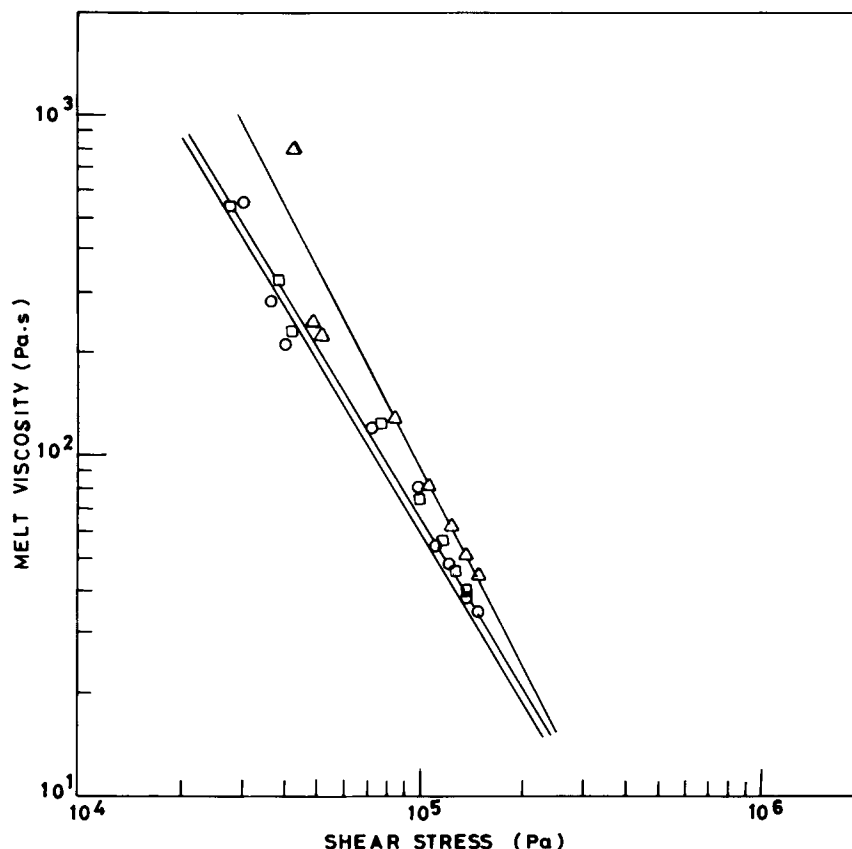


Figure 6 Variation of melt viscosity with shear stress for PP/EVA blend at a constant blending ratio (PP/EVA 90/10) of the matrix and varying VA content (wt %) of the EVA used: (○) 9; (△) 12; (□) 19.

weights of the EVA-12 sample from the other two samples, EVA-9 and EVA-19.

Melt Elasticity

The variation of melt elasticity as a function of shear stress of PP, EVA-12, and their blend is shown in Figure 7 in terms of recoverable shear strain (S_R), which is a parameter most appropriate for characterizing the melt elasticity of multiphase blends.¹ The S_R of EVA is less than that of PP and the PP/EVA blend at shear stresses above 2×10^4 Pa, implying that in their fluid state EVA is less elastic than is PP or the PP/EVA blend at identical temperature and shear stress or shear rate. The magnitude of S_R and its variation with shear stress of the blend differs below and above a critical shear stress ($\tau_c = 1 \times 10^5$ Pa). Below τ_c , the blend has higher melt elasticity than does PP, while at shear stresses above τ_c , the situation is reverse. This suggests the distinct role of EVA in increasing the elasticity of the blend. At τ_c , all the compositions except

one, i.e., 40 wt % EVA content, seem to show identical melt elasticity. Surprisingly, this critical shear stress (viz. 1×10^5 Pa) produces some distinct changes in the morphology of the dispersed phase, as discussed in detail in a subsequent section. Below τ_c , droplet size increases with increasing shear stress, whereas above τ_c , the droplet size decreases with increasing shear stress.

As a function of the blending ratio, the melt elasticity varies, as shown in Figure 8. At any constant shear stress, the variation of S_R is nonlinear, showing two maxima (at 5 and 30 wt % EVA content). At 5 wt % EVA content, S_R of the blend is higher than that for PP at all shear stresses. A further increase of EVA content up to 10 wt % decreases the melt elasticity. This is followed by an increase of melt elasticity with increasing EVA content up to 30 wt % and then a decrease at higher EVA content. This variation of melt elasticity with composition is apparently the effect of morphology of dispersion in the blend, i.e., the size, number density, and shape of the dispersed-phase droplets. As will be shown in

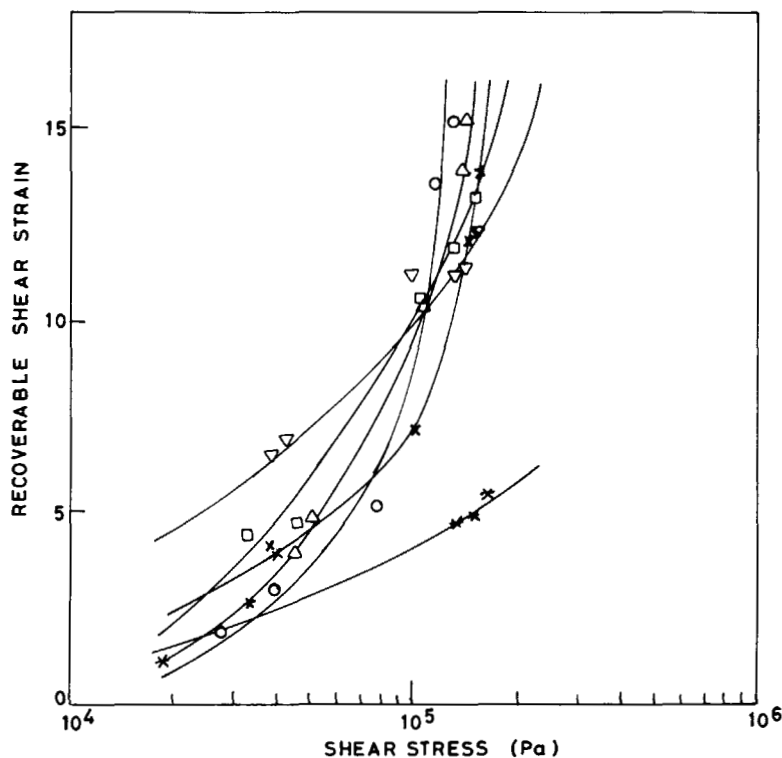


Figure 7 Variation of recoverable shear strain with shear stress for PP/EVA-12 blend at varying compositions (EVA wt %): (○) 0; (△) 10; (□) 20; (▽) 30; (×) 40; (*) 100.

a following section, the droplets increase in number density without any significant change of their average diameter up to 10 wt % EVA content and then increase in size on increasing the EVA content to 20 wt %. At 30 wt % EVA content, the droplet size decreases to about that at 10 wt % EVA content. At 40 wt % EVA content, the droplets coalesce to form bigger droplets, whose deformation under shear is quite different from the smaller droplets, which accounts for the observed low melt elasticity at this composition.

The melt elasticity shows higher values at smaller droplet size (i.e., 5 and 30 wt % EVA content) and lower values at larger droplet size (i.e., 20 wt % EVA). Smaller droplets are less deformable and thus provide better elastic recovery (i.e., an increase of S_R) to the blend. As the droplet size increases, the deformability increases and, hence, the S_R of the blend decreases. This explains the observed behavior of the system in the whole range of blend composition.

The variation of melt viscosity and melt elasticity with composition is similar for blends containing 0–30 wt % EVA content. Melt elasticity of the blend at 40 wt % EVA content decreases, while the melt viscosity increases. This is an effect of the coales-

cence of the EVA droplets, which is mutually opposite on η and S_R . While the big droplets obstruct the flow leading to an increase in the melt viscosity, they are easily deformable, causing a decrease in the melt elasticity.

Morphology

Scanning electron micrographs of etched fracture surfaces of the extrudates of PP/EVA-12 blend at varying blending ratios under two conditions of extrusion, viz. (i) at constant shear stress and (ii) at varying shear stress, are shown in Figures 9 and 10, respectively. These micrographs clearly show the two-phase morphology of the PP/EVA blend, with EVA forming the discrete phase. The size and shape of dispersed-phase domains vary with blending ratio and the shear stress. On etching with toluene at 40°C, the EVA dissolves out, leaving behind the voids that appear black in the micrographs.

(a) Effect of Blend Composition

At a constant shear stress (see the micrographs of Fig. 9), the EVA droplets, which are sufficiently spherical especially at the low EVA contents, are

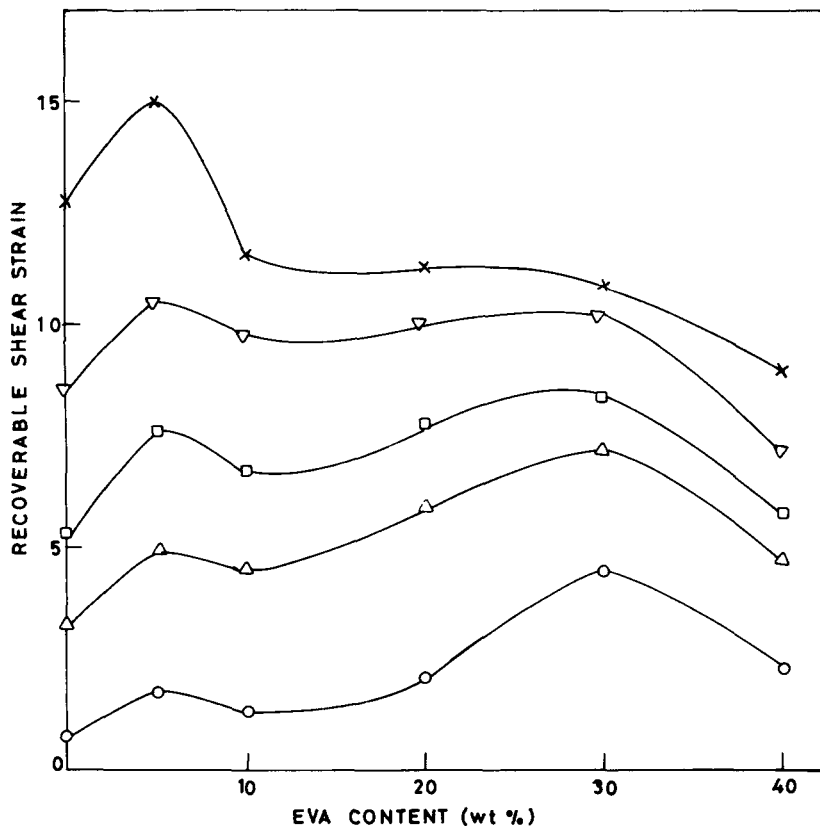


Figure 8 Recoverable shear strain of PP/EVA-12 blend as a function of EVA content (wt %) with shear stress (Pa) as the variable: (○) 2×10^4 ; (△) 5×10^4 ; (□) 7×10^4 ; (▽) 1×10^5 and (x) 1.2×10^5 .

quite homogeneously dispersed in the PP matrix. At high EVA contents, some of the droplets become too large and nonspherical, resembling in appearance the coalescence of smaller droplets. Average diameter, determined after measuring the diameter of about 200 droplets of a given micrograph on a Projectina microscope, and the approximate number of droplets in a given area (i.e., the number density) are shown in Table III. With an increase of the EVA content of the blend from 5 to 10 wt %, the number density of droplets increases while the average droplet diameter shows little variation. At 20 wt % EVA content, there appears a wide distribution of droplet size.

The fraction of large-sized droplets is more at 20 wt % EVA content than at 30 wt % EVA content, as concluded from the respective histograms (not shown here). At this latter composition, the number density of the droplets is distinctly higher (0.78 in arbitrary units) and the average diameter is smaller ($0.39 \mu\text{m}$) than that observed at 20 wt % EVA content (for which the number density and droplet diameter are 0.60 arbitrary units and $0.45 \mu\text{m}$, re-

spectively). This seems to be an effect of shear-induced droplet breakup, which depends upon the rheological properties of the two components and their relative proportion, an effect already recognized by other authors.^{4,18,19} A detailed analysis based on the existing theories, which will be presented in a subsequent publication,²⁰ confirms the observed variation in the size of the dispersed droplets at various compositions of this blend. At 40 wt % EVA content, the morphology changes significantly and the droplets coalesce to form large nonspherical-shaped droplets during processing.

(b) Effect of Shear Stress

The effect of shear stress on the dispersion and size of the dispersed droplets is illustrated for a constant blending ratio (i.e., 20 wt % EVA content) in Figure 10. The droplet diameter, as shown in Table IV, increases from 0.32 to $0.45 \mu\text{m}$ as the shear stress increases from 3.3×10^4 to 4.5×10^4 Pa. Then, with a further increase of shear stress, the droplet diameter decreases to a value $0.26 \mu\text{m}$ continuously

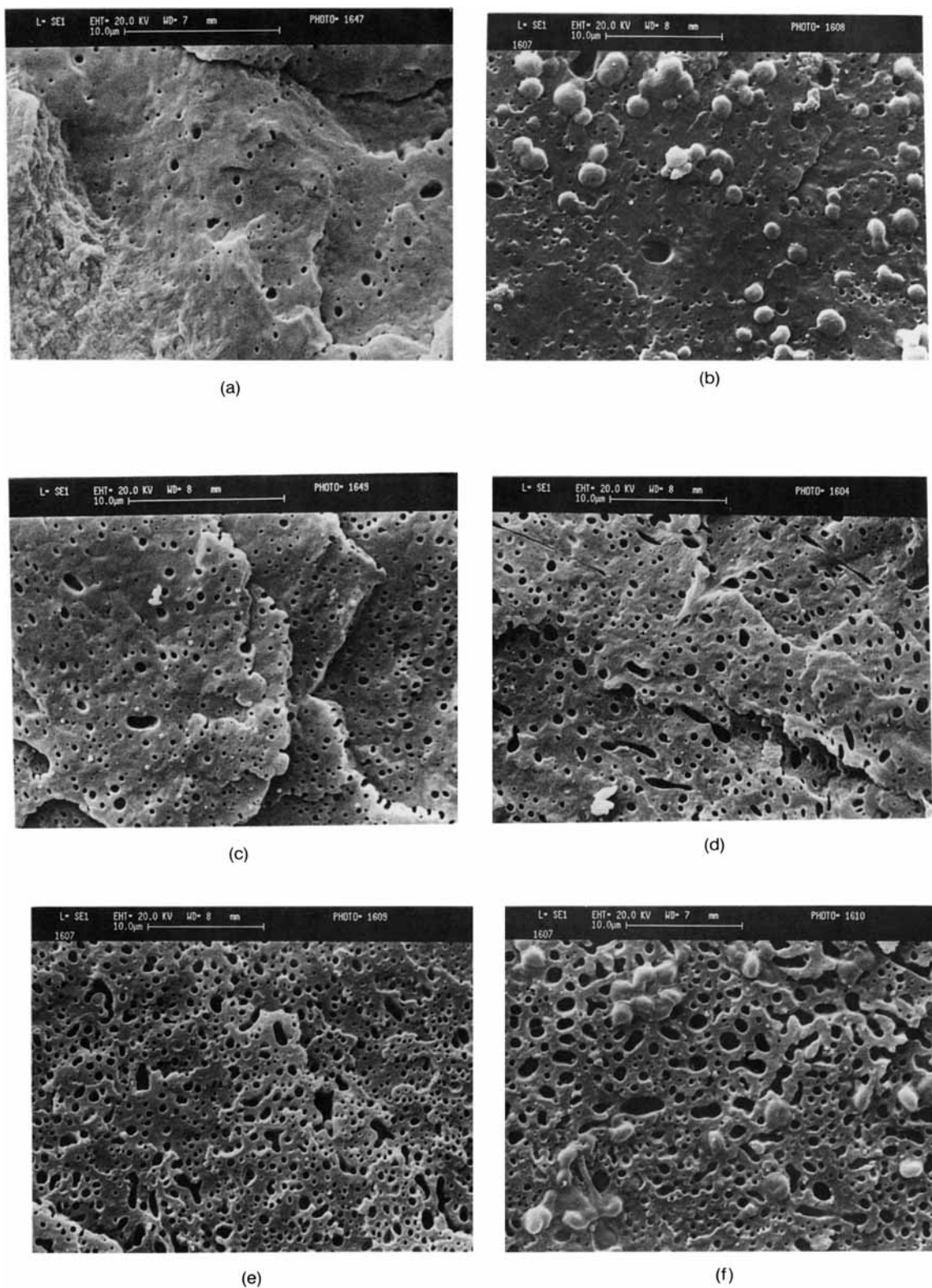


Figure 9 Scanning electron micrographs of rheometer extrudates of PP/EVA blend at a constant shear stress 4.5×10^4 Pa and varying compositions (EVA wt %): (a) 5; (b) 10; (c) 15; (d) 20; (e) 30; (f) 40.

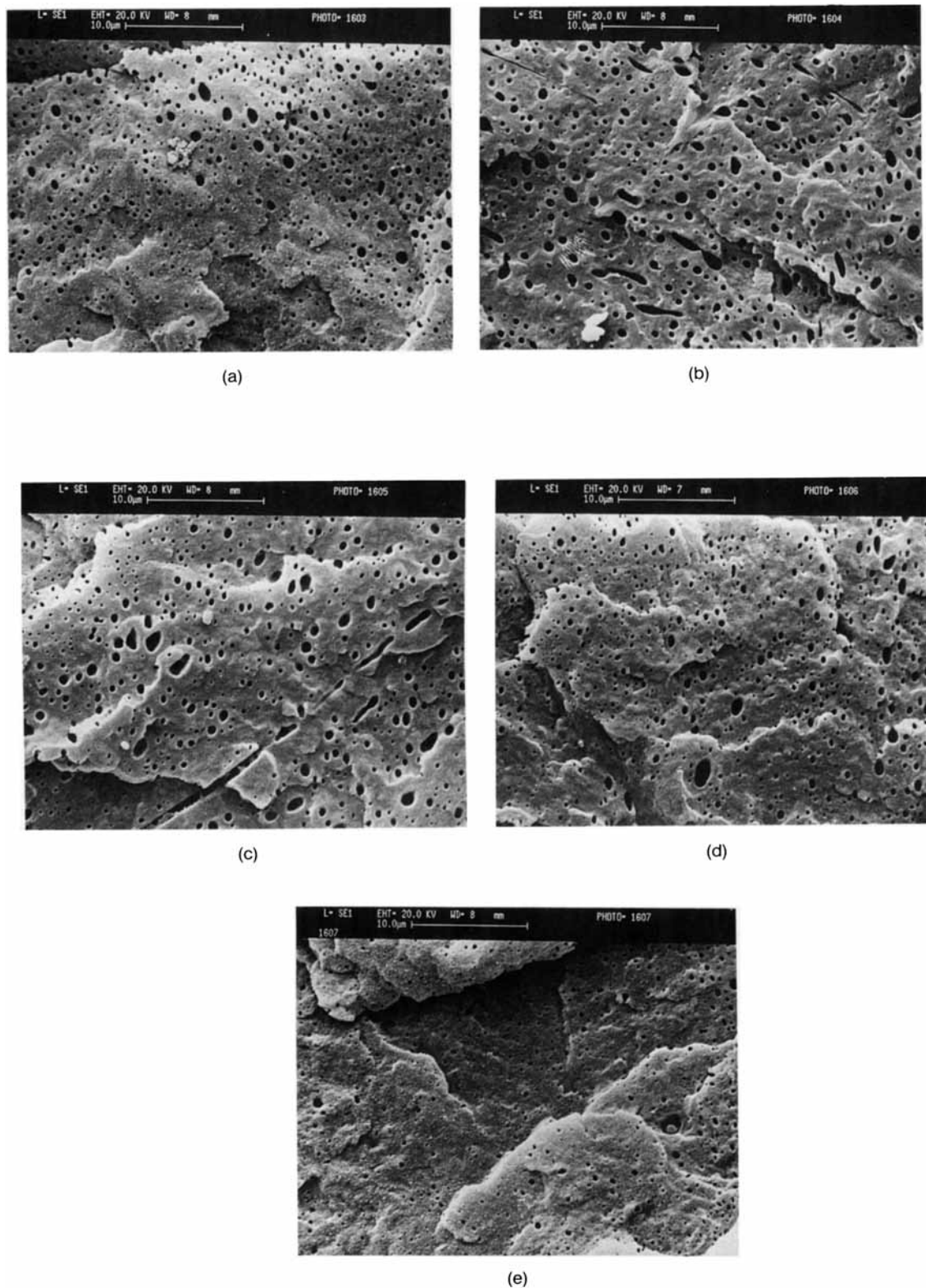


Figure 10 Scanning electron micrographs of rheometer extrudates of PP/EVA-12 80/20 blend at varying shear stress (Pa): (a) 3.3×10^4 ; (b) 4.5×10^4 ; (c) 1.0×10^5 ; (d) 1.3×10^5 ; (e) 1.5×10^5 .

Table III Values of Average Diameter and Number Density of Droplets at Varying Blending Ratios and Constant Shear Stress (4.5×10^4 Pa)

Blend Composition PP/EVA-12	Average Diameter (μm)	Number Density ^a (per unit area)
95/5	0.36	0.26
90/10	0.37	0.44
80/20	0.45	0.60
70/30	0.39	0.78
60/40	0.56	0.48

^a Number of droplets in the micrograph divided by scanned area of the sample.

up to the highest shear stress studied, viz. 1.5×10^5 Pa. This variation of droplet size can be explained in terms of the occurrence of two effects in competition, viz. the coalescing of droplets and shear-induced droplet breakup. Initially, at low shear stress, there is a tendency of the droplets coalescing with other droplets to form bigger ones. This tendency is lower at the lower shear stress (i.e., 3.3×10^4 Pa) than at the next higher shear stress (i.e., 4.5×10^4 Pa). This is obvious because at the lowest shear stress, owing to the extremely slow flow rate, the contact between the droplets would be very infrequent; hence, the chance for coalescing is minimized. The higher shear stress (i.e., 4.5×10^4 Pa) seems quite favorable for this effect, as is apparent from the high values of the mean droplet diameter. As the shear stress increases further, above 4.5×10^4 Pa, the shear-induced droplet breakup effect predominates, which is reflected in the observed decrease of the droplet diameter.

CONCLUSIONS

EVA forms a two-phase blend with PP, showing quite homogeneous mixing and good dispersion of EVA as sufficiently spherical droplets in the PP matrix. The mean diameter of dispersed-phase droplets is not only dependent on the blending ratio but also on the shear stress.

PP, EVA, as well as their blends are pseudoplastic with the power law exponent value between 0.3 and 0.6. Variation of pseudoplasticity of the blend is quite irregular at the lower processing temperature (210°C), while at the higher temperature, a trend is apparent, suggesting that the pseudoplasticity of the blend decreases with increasing EVA content.

Nonlinear variation of melt viscosity with the blending ratio is quite consistent with the changes in the number density and average size of the dis-

persed EVA droplets. The effect of shear stress on melt viscosity is such that below a critical shear stress (i.e., 1.0×10^5 Pa) the blending produces appreciable changes, while above this critical shear stress, the curves for all the blending ratios overlap or converge. It seems that this critical shear stress corresponds to the onset of shear-induced droplet breakup. This critical value of shear stress for shear-induced droplet breakup is also confirmed by the changes in dispersed-phase morphology of this blend. Melt viscosity shows a maximum and minimum at 10 and 20 wt %, respectively, which is attributable to the net result of two mutually competing effects, viz. the predominance of number density and the size of the dispersed EVA droplets in the PP matrix.

At the critical shear stress ($\tau_c = 1 \times 10^5$ Pa), the melt elasticity parameter shows an identical value for all the blending ratios. The maxima and the minima in the melt elasticity are consistent with the changes in mean diameter of the dispersed EVA droplets, such that the larger the droplet diameter the lower is the elasticity of the melt. For the PP/EVA blend (in case of the EVA sample containing 12% VA), a composition corresponding to 20 wt % EVA content seems to be the most appropriate one from the processability point of view. At this composition, both the melt viscosity and melt elasticity are close to their minima observed in the studied range. The morphology of the dispersion also shows uniqueness at this composition of the blend, the average diameter of the dispersed-phase droplets being around $0.35 \mu\text{m}$, which is within the limits stated²¹ for optimum impact toughening of PP by an elastomer. The activation energy of flow is the lowest at this blend composition, which implies greater ease of flow.

Table IV Values of Average Diameter and Number Density of Droplets at Constant Blending Ratios and Varying Shear Stress

Shear Stress (Pa)	PP/EVA (80/20)	
	Average Diameter (μm)	Number Density ^a (per unit area)
3.3×10^4	0.32	0.78
4.5×10^4	0.45	0.60
1.0×10^5	0.37	0.58
1.3×10^5	0.30	0.84
1.5×10^5	0.26	0.69

^a Number of droplets in the micrograph divided by scanned area of the sample.

REFERENCES

1. C. D. Han, *Multiphase Flow in Polymer Processing*, Academic Press, New York, 1981, Chap. 4.
2. C. D. Han, *Rheology in Polymer Processing*, Academic Press, New York, 1978, pp. 169–176.
3. A. P. Plochocki, in *Polymer Blends*, D. R. Paul and S. Newman, Eds., Academic Press, New York, 1978, Vol. 2, Chapt. 21.
4. H. Van Oene, *Polymer Blends*, D. R. Paul and S. Newman, Eds., Academic Press, New York, 1978, Vol. 1, Chap. 7.
5. M. Kreyszewski, T. Pakula, and A. Galeski, *J. Colloid Interface Sci.*, **44**, 85 (1973).
6. L. A. Utracki and M. R. Kamal, *Polym. Eng. Sci.*, **22**, 96 (1982).
7. C. D. Han, Y. W. Kim, and S. J. Chen, *J. Appl. Polym. Sci.*, **19**, 2831 (1975).
8. A. P. Plochocki, *Trans. Soc. Rheol.*, **20**, 287 (1976).
9. J. F. Carley and S. C. Crossan, *Polym. Eng. Sci.*, **21**, 249 (1981).
10. A. K. Gupta and S. N. Purwar, *J. Appl. Polym. Sci.*, **29**, 1079 (1984).
11. A. K. Gupta, P. Krishna Kumar, and B. K. Ratnam, *J. Appl. Polym. Sci.*, **42**, 2595 (1991).
12. A. P. Plochocki, *Polym. Eng. Sci.*, **22**, 1153 (1982).
13. A. P. Plochocki, *Polym. Eng. Sci.*, **23**, 1153 (1983).
14. M. Horio, T. Fuji, and S. Onogi, *J. Phys. Chem.*, **68**, 778 (1964).
15. S. Danesi and R. S. Porter, *Polymer*, **19**, 448 (1978).
16. A. K. Gupta, B. K. Ratnam, and K. R. Srinivasan, *J. Appl. Polym. Sci.*, **45**, 1303 (1992).
17. P. A. Tanguy, L. Choplin, and P. Hurez, *Polym. Eng. Sci.*, **28**, 529 (1988).
18. S. Wu, *Polym. Eng. Sci.*, **27**, 335 (1987).
19. L. Min, J. L. White, and J. F. Fellers, *Polym. Eng. Sci.*, **24**, 1327 (1984).
20. A. K. Gupta, B. K. Ratnam, and K. R. Srinivasan, to appear.
21. B. Z. Jang, D. R. Uhlmann, and J. B. Vander Sande, *J. Appl. Polym. Sci.*, **30**, 2485 (1985).

Received July 8, 1991

Accepted November 14, 1991